Nuclear Instruments and Methods in Physics Research A 865 (2017) 133–138

Contents lists available at ScienceDirect

Nuclear Instruments and Methods in Physics Research A

journal homepage: www.elsevier.com/locate/nima

Transverse beam matching under the influence of space charge

G. Kourkafas[a,*,1], G. Asova[a,2], M. Bakr Arby[a,3], P. Boonpornprasert[a], M. Gross[a], J. Good[a], C. Hernandez-Garcia[a,4], H. Huck[a], D. Kalantaryan[a], M. Krasilnikov[a], O. Lishilin[a], D. Malyutin[b], B. Marchetti[c], A. Matveenko[b], D. Melkumyan[a], M. Otevrel[a,5], Y. Renier[a], T. Rublack[a], F. Stephan[a], G. Vashchenko[a,6], Q. Zhao[a,7]

[a] Deutsches Elektronen-Synchrotron (DESY), Platannenallee 6, 15738 Zeuthen, Germany
[b] Helmholtz-Zentrum Berlin für Materialien und Energie GmbH (HZB), Hahn-Meitner-Platz 1, 14109 Berlin, Germany
[c] Deutsches Elektronen-Synchrotron (DESY), Notkestrasse 85, 22603 Hamburg, Germany

ARTICLE INFO

Keywords:
Transverse matching
Space charge

ABSTRACT

The matching of a particle beam to specific transverse parameters, imposed by various operational, functional and diagnostic reasons, is an essential procedure in most types of accelerators. While well-established methods can easily match beams of negligible self fields, their accuracy is significantly reduced in the presence of strong space-charge forces. In a pursuit of time-efficient matching solutions for space-charge influenced beams, two approaches are demonstrated in this paper: a faster and more approximative one for symmetric beam transport along periodic and dense lattices, and a more analytic one for broader beam and lattice conditions. Beam dynamics simulations and experimental measurements are used to validate the performance of the suggested methods for the matching requirements of the transverse phase–space tomography at the Photo Injector Test Facility at DESY, Zeuthen site (PITZ).

1. Introduction

The operation of most linear and circular particle accelerators requires specific transverse beam parameters to be delivered at certain locations of the beamline. Furthermore, various applications, diagnostics and experiments impose additional constraints on the beam specifications. For example, the tomography of the transverse phase-space is optimized when the beam projections are captured at specific phase-advance values [1], a condition often connected with the delivery of certain incoming Courant–Snyder parameters [2]. The measurement of the longitudinal phase space with a transverse deflecting cavity is improved when a 90° phase advance between the cavity and the measurement station is achieved and the beam size at both locations is minimized [3]. Matching is also necessary for the injection of a beam into undulators used for free-electron-laser (FEL) radiation production [4], as well as into novel accelerating channels, such as plasma wake-field accelerators [5].

In order to achieve these requirements, focusing elements with adjustable strengths are employed in a procedure called beam matching. Specialized software packages are typically used to calculate suitable matching solutions for the fundamental beam dynamics, with the Methodical Accelerator Design (MAD) code [6] being one of the most widespread choices. On the other hand, for applications involving compressed beam dimensions, relatively low energies and high peak currents (photo-injectors, bunch-compressor exits, etc.), the performance of a matching routine depends on the proper consideration of the Coulomb repulsion among the beam's particles, namely the space-charge force.

While the matching of space-charge influenced beams in many facilities is progressively achieved by iterative trials during operation, a more effective strategy is desired. Especially for machines like the Photo Injector Test Facility at DESY, Zeuthen site (PITZ) [7] where no

* Corresponding author.
E-mail address: georgios.kourkafas@helmholtz-berlin.de (G. Kourkafas).
[1] Currently at Helmholtz-Zentrum Berlin für Materialien und Energie GmbH (HZB), Hahn-Meitner-Platz 1, 14109 Berlin, Germany.
[2] On leave from INRNE-BAS, 1784 Sofia, Bulgaria.
[3] Currently at Assiut University, 71516 Assiut, Egypt.
[4] Currently at Jefferson Lab, 12000 Jefferson Avenue, Newport News, VA 23606, USA.
[5] Currently at Brno University of Technology, Antonínská 548/1, 601 90 Brno, Czech Republic.
[6] Currently at Deutsches Elektronen-Synchrotron (DESY), Notkestrasse 85, 22603 Hamburg, Germany.
[7] On leave from Institute of Modern Physics, Chinese Academy of Sciences (IMP, CAS), 730000 Lanzhou, China.

http://dx.doi.org/10.1016/j.nima.2016.10.044
Received 1 August 2016; Received in revised form 22 September 2016; Accepted 24 October 2016
Available online 28 October 2016
0168-9002/

standard mode of operation exists and the machine parameters change constantly, the matching requirements need to be achieved within the short measurement time which is available for each working point of the machine. Since the existing simulation codes with the most realistic beam-dynamics modelling require long computational times for the general case of non-symmetric beams, more approximative—yet accurate—solutions have to be discovered.

This article presents a comprehensive and systematic study, accommodated by simulations and measurements, on how to efficiently include the effect of space charge in the beam matching. Depending on the matching specifications, i.e. the magnetic lattice and the beam parameters and constraints, different approaches are followed to combine reasonable precision with time optimization. The following cases are addressed:

- matching of the phase advance or the rms envelope along periodic lattices of dense focusing (Section 2)
- matching or injection of specific transverse beam parameters along irregular lattices (Section 3).

Both of the above are utilized in the transverse Phase Space Tomography (PST) measurement at PITZ [8,9], making it suitable as a case study. PITZ is a research and development accelerator facility, which mainly focuses on testing, characterizing and optimizing photo-injectors, which are used as high-brightness electron sources at short-wavelength FELs. Equipped with an L-band normal-conducting RF gun and an additional booster cavity, it is able to accelerate electron bunches of 2–24 ps FWHM duration and up to 4 nC charge to an energy up to 25 MeV. It is numerous and versatile diagnostics allow a detailed measurement of the 6-D phase space at various locations along the beamline [10].

2. Matching along periodic and dense lattices

The transport lines in various machines are designed to provide a beam propagation with well-defined specifications, typically an average transverse size or phase-advance increment per lattice cell. When certain conditions apply to such lattices, the beam dynamics without and with the linear space-charge force can be directly correlated. This enables matching codes without any space-charge consideration to provide matching solutions valid for space-charge influenced beams. The theory describing this correlation is summarized below, together with the suggested matching method and its application to the PST lattice at PITZ. The non-linear component of space charge tends to be negligible for such lattices, which usually accommodate quasi-frozen beams.

2.1. Integrating the smooth-approximation theory into non-space-charge matching codes

The dynamics of long round beams with uniform charge distribution and fixed energy along periodic lattices have been studied in details by Reiser [11]. The main point of his so-called smooth-approximation theory is that periodic lattices of dense focusing are able to accommodate a constant average transverse beam size in the presence of linear internal and external electromagnetic fields, by achieving an equilibrium between the two. This beam size, mentioned as the matched beam solution, is preserved as long as it is considerably less than the cell length, its initial slope is zero and the phase advance per cell is less than 90° in the absence of space charge. Since the model uses only linear forces, it assumes a constant beam emittance along propagation. Some basic formulas of the theory's consequences are summarized in the following paragraph.

For a beam with a constant effective (or 4-rms) geometrical emittance $\epsilon = 4\epsilon_{rms}$, the matched beam solution in terms of 2-rms beam size $a = 2a_{rms}$ is given by:

$$ka^2 = \epsilon, \tag{1}$$

where k represents the mean value of the net focusing strength (including the effect of space charge), which is connected to the external focusing strength k_0 via

$$k = \sqrt{k_0^2 - \frac{K}{a^2}}, \tag{2}$$

with K being the generalized beam perveance. The last formula already offers a link between the transverse dynamics with and without the contribution of space charge. Using the dimensionless parameter u:

$$u = \frac{K}{2k_0\epsilon} \tag{3}$$

it is then possible to express the beam's transverse parameters to their non-space-charge components (or zero-current equivalents, denoted with the subscript 0), which are determined only by the external forces. Specifically, the phase advance of each period ϕ, the mean β-function $\overline{\beta}$ and the α-function at the locations where $\beta = \overline{\beta}$ [9] are given by:

$$\phi = \phi_0(\sqrt{u^2+1} - u),\ \overline{\beta} = \overline{\beta_0}(u + \sqrt{u^2+1}),\ \alpha = \alpha_0(u + \sqrt{u^2+1}). \tag{4}$$

With the help of the above equations, the transverse matching can be performed by software routines which neglect space charge (e.g. MAD), provided that the zero-current components of the involved beam parameters are used. The predicted solutions (focusing strength, drift length) will still hold in the presence of self fields, when the actual (space-charge equivalent) beam parameters are considered.

When k_0 is used as a matching variable instead of the lattice length S, it is more convenient to eliminate the first in the expression of the u parameter, using [11]:

$$\phi_0 = \int_z^{z+S} \frac{1}{\beta_0}\,\mathrm{d}z = \frac{S}{\overline{\beta_0}} = Sk_0\,. \tag{5}$$

By combining the above equations, ϕ_0 can be calculated as [9]

$$\phi_0 = \sqrt{\phi^2 + \frac{KS}{\epsilon}\phi}\,, \tag{6}$$

suggesting that for a lattice of constant period length, the description of the space-charge density is given by the generalized perveance and the emittance of the beam. The performance of this approach using the MAD software is demonstrated below for the phase-advance matching at PITZ.

2.2. Phase-advance matching at PITZ

The standard PST measurement at PITZ utilizes three FODO cells (a sequence of quadrupole magnets with alternating polarity separated by equal drift spaces) with the requirement of a 45° phase advance per cell. The effective length of the quadrupoles is 43 mm and the drift space 337 mm, giving a total cell length of 760 mm (more details in [12]). The typical beam parameters create considerable self fields along the PST lattice, where the steep phase-advance increment opposes a transport with very small transverse dimensions [13].

In this study, an electron beam with 1 nC charge, 22 ps duration and 25 MeV/c momentum is matched with MAD to the requirements of the PST lattice, without and with the space-charge consideration. For the latter case, a small (1.1 mm mrad) and a large (3.3 mm mrad) value of normalized rms emittance (ε) is considered for both transverse planes. Given the beam parameters, the lattice length and the requirement of ϕ=45° per cell, ϕ_0 is calculated from Eq. (6) and passed as a matching constraint to MAD. The resulting matching solution (quadrupole strength and zero-current β_0- and α_0-value in the middle of the drift lengths), together with the corresponding β- and α-parameters are presented in Table 1, with the zero-current case represented on top, with a dash in the emittance column.

As expected, stronger focusing is predicted with increasing space-

Table 1
Matching solutions for the studied emittance cases with the corresponding beam parameters.

ε (μm rad)	k_0 (m^{-2})	$\beta_{0x,y}$ (m)	$\alpha_{0x,y}$	u	$\beta_{x,y}$ (m)	$\alpha_{x,y}$
–	48.8	1.00	± 1.13	0.00	1.00	± 1.13
3.3	52.5	0.93	± 1.14	0.08	1.00	± 1.23
1.1	59.2	0.83	± 1.17	0.21	1.02	± 1.44

Table 2
Phase-advance mismatch at the end of each FODO cell when matching a beam of ε = 1.1 mm·mrad without and with the consideration of space charge.

	$\Delta\phi$ **after cell**:		
	#1	**#2**	**#3**
***x*-plane**			
Matching without space charge	−3.1°	−16.9°	−34.5°
Matching with space charge	0.9°	0.9°	−1.2°
***y*-plane**			
Matching without space charge	−4.7°	−20.2°	−37.8°
Matching with space charge	−1.9°	−4.5°	−3.6°

charge density and additionally a smaller β_0 and a bigger α_0. The calculation of the corresponding Courant–Snyder parameters show that the β-function remains practically unchanged regardless the space-charge conditions while a slightly bigger α-function is needed as the space-charge density increases.

The performance of the space-charge matching in comparison to the zero-current approach was evaluated using the ASTRA tracking code [14], which offers a detailed simulation of the beam dynamics, including the self fields. As a figure of merit, the phase-advance mismatch $\Delta\phi$ delivered at the end of each cell with respect to the target value is presented in Tables 2 and 3 for each studied emittance value respectively.

Significant cumulative mismatches are observed when space charge is neglected, up to 38° for the smaller emittance beam which is subject to stronger self fields. On the other side, the space-charge compensating matching practically eliminates the phase-advance mismatch, reducing it below 5°, which is a value created by the fringe fields of the magnets [9]. The scaling predicted by the smooth-approximation theory, as formulated by the u factor, proves to be consistent for both space-charge densities.

The big advantage of this method is the combination of accuracy and computational speed: the scaling of the parameters and the matching with MAD yields almost instant results. However the strict conditions required by this analysis are not met in more general cases, where lattices of aperiodic and sparse focusing are used to match asymmetric beams. More detailed models are then needed for a satisfactory prediction of the beam dynamics, as presented in the following section.

Table 3
Phase-advance mismatch at the end of each FODO cell when matching a beam of ε = 3.3 mm mrad without and with the consideration of space charge.

	$\Delta\phi$ **after cell:**		
	#1	**#2**	**#3**
***x*-plane**			
Matching without space charge	−1.4°	−7.9°	−15.9°
Matching with space charge	−0.1°	−1.4°	−3.4°
***y*-plane**			
Matching without space charge	−2.2°	−9.8°	−17.4°
Matching with space charge	−1.1°	−3.7°	−4.9°

3. Matching along irregular and sparse lattices

In general, injection lines neither provide a dense periodic focusing nor do they accommodate a symmetric and smooth beam transport. Under such conditions, the defocusing effect of space charge is just a part of its implications to the transverse dynamics. A critical consequence of the self fields becomes then the correlated growth of the projected emittance, an effect which has been measured to be dominant along the matching lattice of PITZ [15]. A short explanation of this phenomenon and a tool able to compensate its effect are presented below.

3.1. Matching combined with emittance compensation

As firstly described by Carlsten [16] and thoroughly characterized by Serafini and Rosenzweig [17], a space-charge influenced particle bunch shall not be treated as a whole, but its inhomogeneity along the longitudinal axis has to be taken into account. Even in the case of a longitudinally uniform charge distribution, the longitudinal dependence of the transverse self fields [18] creates focusing conditions which can be considered practically constant only along thin slices of the bunch. Due to this coupling between the longitudinal and the transverse planes, a distinction between sliced and projected (overall) beam dynamics is necessary.

With the different longitudinal slices being subject to different focusing, they end up having different transverse properties. The result is a diffusion of the transverse phase-space along the bunch length, which appears as an increase of the projected emittance, regardless of the much lower emittance of the individual slices. This so-called correlated growth of the projected emittance is a common issue especially in photo-injectors and is overcome via a procedure known as emittance compensation. The latter includes a proper adjustment of the external focusing (typically a solenoid) in order to align the phase-space portraits of the slices and thus minimize the projected emittance in a specific location downstream.

The growth of the projected emittance has a crucial impact on the matching efficiency, since it directly affects the beam transport and the delivered parameters. For this reason, matching codes which assume a constant beam emittance (e.g. MAD) are not able to deliver accurate results in such cases. Moreover, the matching goals are expected to be delivered all along the bunch length, rather than in just parts of it or averaged over a longitudinally incoherency. Therefore, an effective matching procedure needs to additionally perform emittance compensation—extended into the 2-D symmetry plane for compliance with the quadrupole fields and the matching constraints. These exact features are implemented in the Space Charge Optimizer code, as explained below.

3.2. The space charge optimizer code

Based on the theoretical work of Miginsky [19], Matveenko and Bondarenko developed the Space Charge Optimizer (SCO) software [20] in order to provide a 2D-emittance compensation scheme for the injector of the Berlin Energy Recovery Linac Project, bERLinPro, at Helmholtz-Zentrum Berlin. SCO resembles in its operation most of the common tracking and matching codes: it requires an input beam, a beamline description and a definition of the matching requirements. Its major advantage though is that the input beam is not treated as a whole, but is divided into a user-defined number of longitudinal slices. For each of these slices, the beam envelope equation for both transverse planes is solved numerically, including the linear self fields. In this way, each longitudinal slice contributes to the calculation of the projected emittance, yielding very fast results in the same time. This approach is very similar to the one followed by HOMDYN [21], a code developed to match photo-injector beams into further accelerating stages.

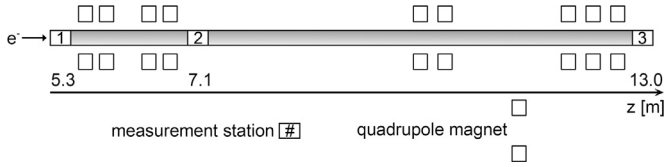

Fig. 1. Schematic layout of the matching lattice used for the PST measurement at PITZ. Nine matching quadrupoles are located among three transverse emittance measurement stations, the longitudinal position of which is indicated on the coordinate axis below.

For the calculation of the matching solution, SC uses an iterative algorithm which seeks to minimize the user-influenced cost function, while tracking each intermediate result. The parameters which can be given as constraints currently are the projected emittance, the α- and β-functions of both transverse planes at the end of the lattice, as well as the maximum transverse rms size along the whole lattice. Various optimization options are available in order to vary the accuracy of the result, in the expense of computational complexity.

The capabilities of SCO fit exactly to the needs of the matching section at PITZ. Its performance is demonstrated below, using simulated and experimental data.

3.3. Validation with experimental results and simulations at PITZ

The matching section at PITZ consists of a series of quadrupoles, positioned in a non-regular way among the diagnostics of the high-energy section. For the case of the PST measurements in 2015, nine quadrupole magnets were utilized between the first transverse phase-space measurement station (z=5.3 m) and the entrance of the PST lattice (z=13.0 m), as schematically shown in Fig. 1. An additional measurement station is located after the fourth quadrupole, employing the slit-scan measurement technique just like the first station. The matching aim is to reach the Courant–Snyder parameters shown in Table 1 at the entrance of the PST lattice, while minimizing the projected emittance in the same time.

The SCO software was used to match a beam of 21.0 MeV/c momentum and 500 pC bunch charge, generated with 12 ps FWHM long laser pulses of Gaussian profile. For the description of the input beam, the transverse projected rms moments were measured at the beginning of the matching lattice (z=5.3 m), after tuning the machine settings to approach emittance compensation at that location (the strength of the solenoid in the low-energy section was tuned to the value which minimized the measured projected emittance). In this way, the measured parameters (first column in Table 4) are assumed to characterize every longitudinal slice of the bunch. Using optimization parameters which by experience achieve satisfactory convergence relatively quickly (< 20 min with a conventional computer), SCO calculated the solution plotted in Fig. 2a.

An off-line simulation of this solution with ASTRA, using a distribution of $5{\cdot}10^5$ macroparticles with gaussian profile (upper left plots in Figs. 3 and 4) and a 3-D space-charge grid of 25 ×25 × 29, yields the transport plotted in Fig. 2b after ~3.5 h simulation time. The resulting peaks correspond to the known feature of the emittance calculation within quadrupoles by ASTRA [14] and should be ignored. A remarkable similarity is observed between the results of the two tracking methods despite their incomparable difference in simulation speed, indicating the minor effect of the non-linear space-charge forces in the overall beam dynamics. Complementary simulations with bunch charges from 100 pC to 1 nC support this observation [9].

This agreement is confirmed by the measured trace-space portraits using the slit-scan technique (2nd station) and the tomographic reconstruction (3rd station), which are presented in Figs. 3 and 4 for each transverse plane alongside with the simulation results from ASTRA. Taking into account the approximative representation of the measured distribution in the simulation, the evolution of the trace space follows quite closely the predicted one. The measurement results at the last station, which employs the PST technique with four projection screens, have to undergo a 10% intensity cut in order to diminish the reconstruction artefacts without compromising the main beam features, according to empirical and simulation studies [8,22]. Apart from that, the beam widening measured at this location is due to the higher signal-to-noise ratio of the PST measurement [8], making it more susceptible to the beam halo, which grows downstream and has not been included in the ideal distribution of the simulation.

In more quantitative terms, Table 4 summarizes the simulated and measured beam parameters. A reasonable accordance is observed between the simulated and the measured Twiss parameters at both locations and transverse planes. The delivered mismatch is considered well acceptable and by far better than in the case of constant-emittance approaches, when it can climb up to several hundreds per cent even when the self fields are included. This result becomes even more important when taking into consideration the relatively short time of the matching optimization and the machine imperfections during the measurement (instability of the cooling system, strong inhomogeneity of the transverse laser profile, not optimized beam trajectory). When focusing on the value of the normalized emittance, the agreement between simulation and measurement is not as good as for the other two parameters, especially at the final location. Besides the different measurement technique and the contribution of the beam halo explained above, this discrepancy is intensified by the approximation of the initial beam distribution in the simulation, which neglects the irregularities of the actual trace space and thus suppresses potential sources of emittance growth such as the transverse coupling, non-linear fields, etc.

4. Conclusions

The incorporation of space charge into the transverse beam matching in a time-efficient way has been addressed in this article. Depending on the complexity of the boundary conditions, two different approaches were suggested and evaluated with simulated and experimental data from PITZ. For symmetrical stationary beams propagating along lattices of periodic and dense focusing, traditional matching codes with no space-charge consideration can be combined with the smooth-approximation theory to match the phase advance or the rms envelope almost instantly. For more general lattice and beam condi-

Table 4
Transverse beam parameters along the matching lattice of PITZ according to SCO, ASTRA and the measurement, including the statistical errors.

	Measurement station 1	**Measurement station 2**			**Measurement station 3**		
	Measured	SCO	ASTRA	Measured	SCO	ASTRA	Measured
β_x (m)	6.67 ± 0.35	2.08	1.99	2.83 ± 0.11	0.91	1.01	0.78 ± 0.02
α_x	−0.90 ± 0.15	1.09	1.16	1.42 ± 0.10	1.13	0.96	0.70 ± 0.02
$\varepsilon_{n,x}$ (mm mrad)	0.81 ± 0.03	0.86	0.85	0.94 ± 0.04	0.83	0.85	1.96 ± 0.03
β_y (m)	8.54 ± 0.95	4.83	4.80	5.51 ± 0.37	1.03	1.10	1.07 ± 0.01
α_y	−0.60 ± 0.39	2.29	2.39	3.13 ± 0.14	−1.12	−1.15	−1.09 ± 0.02
$\varepsilon_{n,y}$ (mm mrad)	0.88 ± 0.02	0.92	0.91	1.25 ± 0.07	0.89	0.90	1.44 ± 0.02

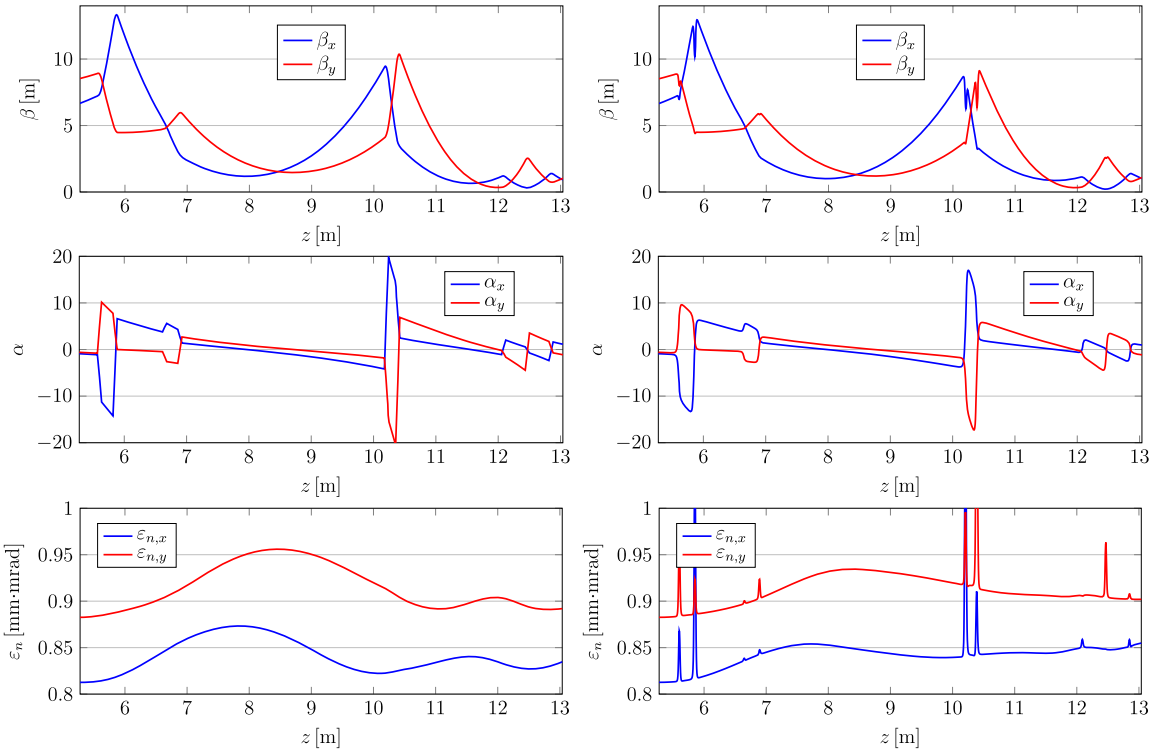

(a) SCO tracking. (b) ASTRA tracking.

Fig. 2. Evolution of the β-function (top), α-function (middle) and normalized emittance (bottom) of the horizontal (blue line) and the vertical plane (red line) along the matching lattice, according to SCO (left) and ASTRA (right). (For interpretation of the references to colour in this figure caption, the reader is referred to the web version of this paper.)

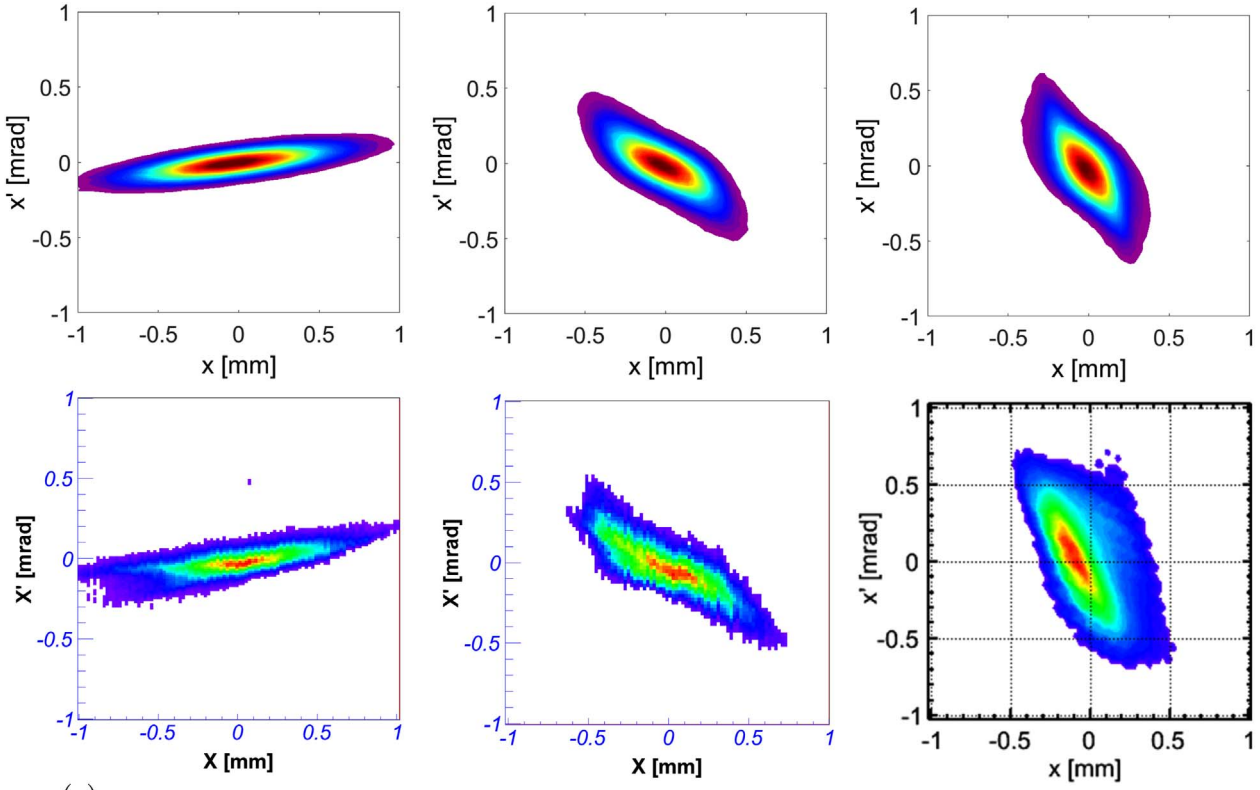

(a) Measurement station #1 (slit-scan). (b) Measurement station #2 (slit-scan). (c) Measurement station #3 (tomography).

Fig. 3. Simulated (top) and measured (bottom) horizontal trace-space distributions at the three measurement stations. The colour code represents normalized charge density (maximum is red, minimum is violet). (For interpretation of the references to colour in this figure caption, the reader is referred to the web version of this paper.)

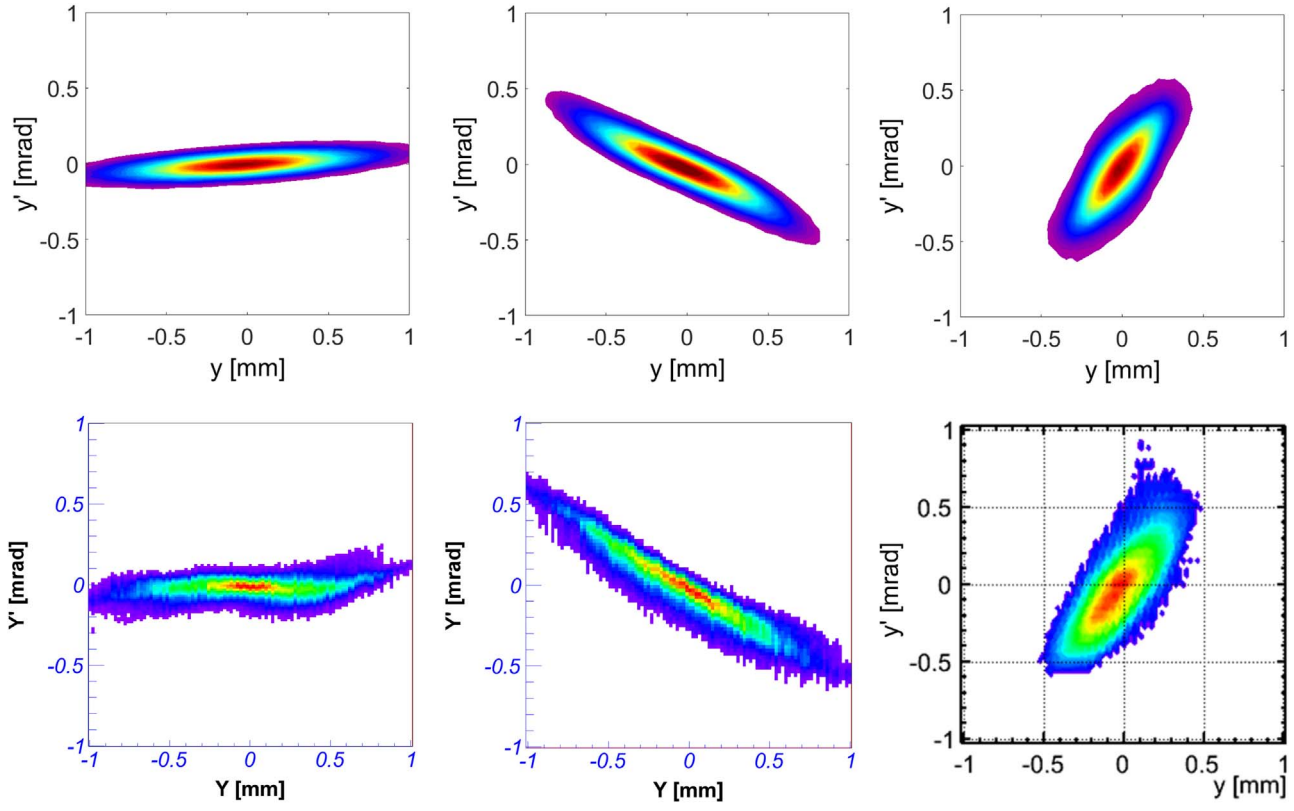

(a) Measurement station #1 (slit-scan). (b) Measurement station #1 (slit-scan). (c) Measurement station #3 (tomography).

Fig. 4. Simulated (top) and measured (bottom) vertical trace-space distributions at the three measurement stations. The colour code represents normalized charge density (maximum is red, minimum is violet). (For interpretation of the references to colour in this figure caption, the reader is referred to the web version of this paper.)

tions, the implementation of the linear self fields on a longitudinally sliced bunch offered by the SCO software is able to match specific beam parameters with acceptable accuracy in a reasonable time frame. The derived results can be especially useful for machines and applications which require beam matching and 2-D emittance compensation under high intensities and condensed beam dimensions, such as photo-injectors, bunch compression regions and undulator entrances.

References

[1] K. Hock, et al., Beam tomography research at Daresbury Laboratory, Nucl. Instrum. Methods Phys. Res. A 753 (0) (2014) 38–55. http://dx.doi.org/10.1016/j.nima.2014.03.050.

[2] E. Courant, H. Snyder, Theory of the alternating-gradient synchrotron, Ann. Phys. 3 (1) (1958) 1–48. http://dx.doi.org/10.1016/0003-4916(58)90012-5.

[3] K. Floettmann, V.V. Paramonov, Beam dynamics in transverse deflecting rf structures, Phys. Rev. ST Accel. Beams 17 (2014) 024001. http://dx.doi.org/10.1103/PhysRevSTAB.17.024001.

[4] L. Giannessi, et al., Self-amplified spontaneous emission for a single pass free-electron laser, Phys. Rev. ST Accel. Beams 14 (2011) 060712. http://dx.doi.org/10.1103/PhysRevSTAB.14.060712.

[5] T. Mehrling, et al., Transverse emittance growth in staged laser-wakefield acceleration, Phys. Rev. ST Accel. Beams 15 (2012) 111303. http://dx.doi.org/10.1103/PhysRevSTAB.15.111303.

[6] Methodical Accelerator Design (MAD), ⟨http://mad.web.cern.ch/mad⟩.

[7] F. Stephan, et al., Detailed characterization of electron sources yielding first demonstration of European X-ray Free-Electron Laser beam quality, Phys. Rev. ST Accel. Beams 13 (2010) 020704. http://dx.doi.org/10.1103/PhysRevSTAB.13.020704.

[8] G. Asova, Tomography of the electron beam transverse phase space at PITZ, (Ph.D. thesis), INRNE, Bulgarian Academy of Sciences, Sofia (2011).

[9] G. Kourkafas, Incorporating space charge in the transverse phase space matching and tomography at PITZ, (Ph.D. thesis), Universität Hamburg, 2015.

[10] M. Krasilnikov, et al., Experimentally minimized beam emittance from an L-band photoinjector, Phys. Rev. ST Accel. Beams 15 (2012) 100701. http://dx.doi.org/10.1103/PhysRevSTAB.15.100701.

[11] M. Reiser, Theory and design of charged particle beamsWiley Series in Beam Physics and Accelerator Technology, Wiley, 1994.

[12] G. Kourkafas, et al., Tomography module for transverse phase-space measurements at PITZ, in: DITANET2011, Seville, Spain, 2011.

[13] G. Kourkafas, et al., The effect of space charge along the tomography section at PITZ, in: Proceedings of IBIC2013, Oxford, UK, 2013, pp. 255 – 258.

[14] A Space charge TRacking Algorithm (ASTRA),⟨http://www.desy.de/~mpyflo⟩.

[15] G. Kourkafas, et al., Emittance increase and matching along the tomography module at PITZ, in: Proceedings of IPAC2014, Dresden, Germany, 2014, pp. 1144–1146.

[16] B. Carlsten, New photoelectric injector design for the Los Alamos National Laboratory XUV FEL accelerator, Nucl. Instrum. Methods Phys. Res. A 285 (12) (1989) 313–319. http://dx.doi.org/10.1016/0168-9002(89)90472-5.

[17] L. Serafini, J.B. Rosenzweig, Envelope analysis of intense relativistic quasilaminar beams in rf photoinjectors: A theory of emittance compensation, Phys. Rev. E 55 (1997) 7565–7590. http://dx.doi.org/10.1103/PhysRevE.55.7565.

[18] M. Ferrario, Accelerator physics: basic principles on beam focusing and transport, in: International School of Physics Enrico Fermi, Course CLXXIX, Laser Plasma Acceleration, Varenna, 20–25 June 2011.

[19] S. Miginsky, Space charge effect, coherence of charge oscillations, and emittance, Tech. Phys. 53 (9) (2008) 1197–1208. http://dx.doi.org/10.1134/S1063784208090119.

[20] A. V. Bondarenko, A. N. Matveenko, Implementation of 2D-emittance compensation scheme in the BERLinPro injector, in: Proceedings of FEL2011, Shanghai, China, 2011, pp. 564–567.

[21] M. Ferrario, et al., HOMDYN study for the LCLS RF photo-injector, in: SLAC-PUB-8400, March 2000, LCLS-TN-00-04, LNF-00/004 (P).

[22] F. Löhl, Measurements of the transverse emittance at the VUV-FEL, Master's thesis, Universität Hamburg, 2005.